Kinetics of Shape Fluctuations in Nanoparticles: An Argument Against the Room-Temperature Kirkendall Effect

J. Erlebacher[1*], D. Margetis[2]

[1]Johns Hopkins University, Materials Science and Engineering, Baltimore, MD 21218

[2]University of Maryland, Mathematics and Institute for Physical Science and Technology, and Center for Scientific Computation and Mathematical Modeling, College Park, MD 20742

*corresponding author

Abstract

   Shape fluctuations in nanoparticles strongly influence their stability. Here, we introduce a quantitative model of such shape fluctuations and apply this model to the important case of Pt-shell/transition metal-core nanoparticles. By using a Gibbs distribution for the initial shapes, we find that there is typically enough thermal energy at room temperature to excite random shape fluctuations in core/shell nanoparticles, whose amplitudes are sufficiently high that the cores of such particles are transiently exposed to the surrounding environment. If this environment is acidic and dissolves away the core, then a hollow shell containing a pinhole is formed; however, this pinhole quickly closes, leaving a hollow nanoparticle. These results favorably compare to experiment, much more so than competing models based on the room-temperature Kirkendall effect.

There are a number of recent observations of hollow nanoparticles formed via the Kirkendall effect in annealed core-shell nanoparticles [1]. The origin of this effect is uncompensated high-temperature bulk diffusion between the core and the shell, i.e., if A is the component in the core, and B is the component of the shell, then the diffusivity of a minority of A in B differs from the diffusivity of a minority of B in A and intermixing requires injection of vacancies at the exterior surface, which diffuse and collect in the core. This effect is certainly operative in many annealed core-shell nanoparticles, because the final shell composition is an alloy mixture of the two components [2]. Recently, however, the Kirkendall effect has been implicated in the formation of hollow Pt-shell nanoparticles formed from Pt-shell, transition metal (e.g., Ni) core nanoparticles in electrolytes at room temperature [3]. This class of nanoparticles is useful in many low-temperature electrochemical reactions, such as oxygen reduction in fuel cells. This "room temperature Kirkendall effect" (rt-KE) is invoked in systems that differ from the high-temperature phenomena in an important way: the shell that is observed to remain after electrochemical processing, which serves to dissolve away any surface Ni, is comprised of pure Pt.

In this Letter, we argue that the kinetics of vacancy-mediated diffusion in core-shell nanoparticles at room temperature are far too slow to justify attribution of the formation of Pt-shell hollow nanoparticles in electrochemical environments to the rt-KE. We present an alternative model (Fig. 1) in which thermal energy induces surface-diffusion mediated random fluctuations in the shape of Pt-shell nanoparticles, fluctuations whose amplitudes are high enough to expose the core, forming pinholes in the shell and allowing the cores to be dissolved away. Once the cores are dissolved away, the mismatch of interior and exterior curvatures provides a new driving force for surface diffusion through the pinholes that closes them rapidly.

In early studies of dealloying (dissolving the less noble component out of a two-component alloy), it was hypothesized that the less noble component might be transported to the surface via a bulk vacancy diffusion mechanism [4]. However, the site concentration of vacancies, $e^{-\Delta G_v/k_B T}$, where ΔG_v is the vacancy formation energy ($\Delta G_v = 1.15$ eV for Pt), is orders of magnitude too low at room temperature (1 vacancy per 3×10^{19} atoms; equivalent to one vacancy in 8×10^{14} 10 nm-diameter Pt nanoparticles) [5]. Similarly, the bulk migration energy (~1.5 eV) yields bulk diffusion coefficients of order 10^{-27} cm^2/sec [6]; this is geologically slow in comparison to the

minutes timescale of the rt-KE. To account for higher vacancy concentrations in Pt-shell particles in acid electrolytes, it is hypothesized that experimental procedures lead to an excess of vacancies at the core/shell interface; similarly, fast vacancy diffusion can be induced in simulation, but only by imposing unrealistically high driving forces [7]. Dealloying has subsequently been shown to be controlled by surface diffusion [8], so it is reasonable to explore whether a similar mechanism can be invoked for core-shell nanoparticles at room temperature, without resorting to the rt-KE.

We start with a deterministic model of nanoparticle shape evolution. The cause of shape changes in a nanoparticle is distinct from the kinetic growth problem of Mullins and Sekerka [9], in which fluctuations in the surface of particles grow because of coupled thermal and concentration gradients. In contrast, in our model the nanoparticle volume is constant, fixed by the equilibrium (spherical) shape. We focus on small fluctuations around this equilibrium shape. Such small fluctuations have long been observed in experiment [10], and resemble vesicle deformations analyzed as a free-boundary problem [11]. We assume uniform surface energy γ, leading to a spherical Wulff shape. The assumption regarding kinetics is that the shape evolves only via surface diffusion, so that the normal velocity v_n of the surface is [12]

$$v_n = -M\Delta_S\kappa .$$ (1)

Here, $\kappa = (\kappa_1 + \kappa_2)/2$ is the mean curvature (the arithmetic mean of principal curvatures κ_1 and κ_2), Δ_S is the surface Laplacian, and $M = C_{surf}D\Omega^2\gamma/k_BT$ is the mobility associated with surface diffusion, where C_{surf} is the areal concentration of diffusers, D is the surface diffusion coefficient and Ω is the atomic volume.

Our approach relies on using Eq. (1) with random initial nanoparticle shapes. We consider an ensemble of initial axisymmetric shapes that form small perturbations of a sphere of radius R_0; these remain axisymmetric by evolution under Eq. (1). In the spirit of [11], let $\rho(s,t)$ be the distance of any point on the surface from the axis (say, z−axis) of rotation, where s is the arc length of the contour that generates the surface and t is time; $0 \le s \le s_m(t)$ and $\rho(s_m(t),t) = 0$. Initially (at $t = 0$), $\rho = R_0 \sin(s/R_0) + \varepsilon\psi_0(s)$, $0 < \varepsilon \square 1$; as a result, we expect

3

that at any later time, $t > 0$, $\rho(s,t) = R_0 \sin(s/R_0) + \varepsilon \psi^{(1)}(s,t) + \varepsilon^2 \psi^{(2)}(s,t) + \cdots$, where each $\psi^{(k)}$ ($k = 1, 2, \ldots$) has units of length. For our purposes, it suffices to compute only $\psi^{(1)}(s,t)$, which we determine via the mean curvature expansion $\kappa(s,t) = 1/R_0 + \varepsilon \kappa^{(1)}(s,t) + \cdots$. By Eq. (1), this $\kappa^{(1)}(s,t)$ satisfies [11] $\partial_t \kappa^{(1)} = -(M/2)[\Delta_0^2 + 2R_0^{-2}\Delta_0]\kappa^{(1)}$, where Δ_0 is the Laplacian on the sphere of radius R_0, $\Delta_0 = \partial_{ss} + R_0^{-1} \cot(s/R_0)\partial_s$, $0 \le s \le \pi R_0$ and ∂_s denotes the partial derivative $\partial/\partial s$. We apply an expansion of $\kappa^{(1)}$ in spherical harmonics $Y_{l0}(\theta)$ with mode amplitudes K_l viz.,

$$\kappa^{(1)}(s,t) = R_0^{-2} \sum_{l=2}^{\infty} K_l Y_{l0}(\theta) e^{-\alpha_l^2 Mt/(2R_0^4)}, \tag{2}$$

where $\alpha_l^2 = (l-1)l(l+1)(l+2)$, $l \ge 2$ and $0 \le \theta = s/R_0 \le \pi$ (θ: polar angle). By definition of the mean curvature, we obtain $\partial_{\theta\theta}\psi^{(1)} + \psi^{(1)} = -2R_0^2\kappa^{(1)}\sin\theta$, which yields the time-dependent shape of the perturbed particle [11]:

$$\psi^{(1)}(s,t) = \sum_{l=2}^{\infty} C_l \hat{\psi}_l(\theta) e^{-\alpha_l^2 Mt/(2R_0^4)}, \quad C_l = -2K_l; \tag{3}$$

C_l has units of length and the (non-dimensional) $\hat{\psi}_l(\theta)$ is the lth-mode shape function,

$$\hat{\psi}_l(\theta) = -\cos\theta \int_0^\theta Y_{l0}(\theta')\sin^2\theta' d\theta' + \sin\theta \int_0^\theta Y_{l0}(\theta')\sin\theta'\cos\theta' d\theta'. \tag{4}$$

Equations (3) and (4) describe the leading-order correction for the shape function *given* the amplitudes C_l, which can be extracted from $\psi_0(s)$ or $\kappa^{(1)}(s,0)$. Stochastic fluctuations in $\psi^{(1)}(s,t)$ are induced by imposing random C_l via the Gibbs distribution. By writing the total energy of the perturbed particle as $E(t) = 4\pi R_0^2 \gamma + \mathcal{E}(t)$, where $\mathcal{E}(0)$ depends on $\psi_0(s)$, we assume that the probability distribution of initial shapes $\psi_0(s)$, or mode amplitudes $\{C_l\}_{l=2}^{\infty}$, is $\mathcal{P}[\psi_0] = Z e^{-\mathcal{E}(0)/(k_B T)}$ (Z: normalization constant). The statistics of shape fluctuations then stem from Eq. (3). To express $\mathcal{P}$ in terms of $\{C_l\}_{l=2}^{\infty}$, consider the formula [12]

4

$\dot{E} \equiv dE(t)/dt = -2\gamma \iint_S v_n \kappa dS$, where S is the nanoparticle surface. By Eqs. (1) and (2), we

compute $\dot{E}(t) \approx -2\varepsilon^2 M \gamma \iint_S \left| \nabla_S \kappa^{(1)} \right|^2 dS = -\varepsilon^2 \left(M\gamma/R_0^4 \right) \sum_l \left[l(l+1)/(2l+1) \right] C_l^2 e^{-\alpha_l^2 Mt/R_0^4}$, which

is integrated to yield

$$\mathcal{E}(t) \approx \gamma \sum_{l=2}^{\infty} \left[(2l+1)(l-1)(l+2) \right]^{-1} C_l^2 e^{-\alpha_l^2 Mt/R_0^4} . \tag{5}$$

In the (equilibrium) limit, $E(t \to \infty) = 4\pi R_0^2 \gamma$, we recover the surface energy of the unperturbed

shape (the sphere). In Eq. (5), we set $\varepsilon = 1$, requiring that C_l be small compared to R_0.

By the Gibbs distribution $\mathcal{P} = Z e^{-\mathcal{E}(0)/(k_B T)}$ with Eq. (5), $\mathcal{P} = \prod_l \mathcal{P}_l$, where

$\mathcal{P}_l \propto e^{-\gamma \left[(2l+1)(l-1)(l+2) \right]^{-1} C_l^2 / (k_B T)}$. Thus, the random fluctuation amplitudes C_l are independent, each

with zero mean ($\langle C_l \rangle = 0$) and variance $\langle C_l^2 \rangle = (1/2)(2l+1)(l-1)(l+2)k_B T/\gamma$. In order for the

linear theory to hold, a reasonable criterion is that $(1/2)\sqrt{\langle C_l^2 \rangle} < R_0$, so we expect that this linear

model is valid for modes l such that

$$l < N \equiv \left(4\gamma R_0^2 / k_B T \right)^{1/3} . \tag{6}$$

Equation (5) indicates that, for fixed perturbation amplitude C_l, the probability $\mathcal{P}_l$ of finding the

lth fluctuation mode increases with l. This is expected physically, as high-l modes are

associated with high spatial frequency fluctuations that require short-distance mass transport.

However, for the problem at hand concerning the rt-KE, analysis of the lowest-mode fluctuations

is most relevant. An argument for this is simply that there is enough thermal energy to indeed

excite the less (relatively) probable fluctuation modes. By the exponential in Eq. (5), the lifetime

of the lth mode is estimated as $\tau_l = R_0^4 M^{-1} \alpha_l^{-2}$, and we can calculate this by using experimental

values for the parameters.

In electrochemical experiments involving Pt-shell nanoparticles, the exterior surface of the

particles is often cycled between potentials that form a surface oxide, leaving a surface

comprised of PtO, and reducing potentials that leave a pure Pt surface. Values for the surface

energies of Pt, PtO, and all other relevant parameters are listed in Table 1 (from [13] and [14],

5

and references therein). We will focus our discussion on particles with radius near $R_0 = 6.5$ nm and shell thickness of 2 nm, at room temperature ($T = 298$ K), comparing to the data of Wang, et al. [3]. For these parameters, Eq. (6) yields an upper bound for l near $N \approx 25$ (for PtO). Independent experimental measurements of C_{surf} and D have not been made. However, Martinez Jubrias, et al. [14] experimentally measured the morphological relaxation times for roughened Pt surfaces as a function of temperature and electrochemical potential, yielding a range for the product DC_{surf} from 0.023 to 0.44 $\sec^{-1}$ over relevant electrochemical potentials from ~0.1 V (Pt) to ~1.1 (PtO) vs. RHE (RHE: reversible hydrogen electrode) [15]. It is important to note that the PtO surface is significantly more mobile than Pt.

Figure 2 shows the probability $\mathcal{P}_l$ of fluctuation versus mode number l for different amplitudes C_l, assuming the Gibbs distribution $\mathcal{P} \propto e^{-\mathcal{E}(0)/(k_B T)}$ for the initial shapes, cf. Eq. (5). For an amplitude of $C_l = 0.5$ nm (i.e., an ~1 nm thick shell), $\mathcal{P}_l$ rises to nearly unity by $l \approx 10$ for both Pt and PtO surfaces. Even for an amplitude of $C_l = 2.0$ nm (an ~4 nm thick shell), the probability $\mathcal{P}_l$ is greater than 40% at $l \approx 10$, although the probability is lower for Pt surfaces.

When a fluctuation on the surface appears with an amplitude such that the core is exposed, then two events can occur depending on the electrochemical potential. If the electrochemical potential is high, then the core will be dissolved away; if the potential is low, dissolution may be slow, and the core and surface components can mix via surface diffusion as the fluctuation decays. At high potentials, dissolution of the core of 10 nm diameter particles is typically faster than one second. For such dissolution to occur, the fluctuation lifetime must be longer. Recall that the lth mode lifetime is $\tau_l = R_0^4 M^{-1} \alpha_l^{-2}$. The lifetime τ_l versus l is plotted in Fig. 3 for Pt- and PtO-terminated surfaces. For nearly all modes, the lifetime of fluctuations is greater than one second (with a still-high existence probability), rising to greater than 10^4 seconds for the very lowest mode ($l = 2$) on Pt-terminated surfaces. Certainly for thin shells ($C_l = 0.5$ nm), we conclude that under reasonable conditions fluctuations are always long enough-lived to expose the core to the surrounding electrolyte, allowing the cores to be dissolved away. For thick shells $\left(C_l = 2.0 \text{ nm} \right)$, while the probability of the fluctuation is near unity on PtO surfaces (high potential), the probability drops off for the lower modes. This is a reflection of the observation

that the PtO surface is significantly more mobile than Pt, and may explain why the hollow Pt shell nanoparticles in Co_3Pt nanoparticles are seen only when the particles are subjected to high potential [16]. Regardless, for surfaces that are comprised of Pt, the model predicts that the shell must be quite thick in order to avoid a fluctuation that will expose the core to an acidic electrolyte able to dissolve it away.

To this point we have argued that pinholes in the nanoparticle shells are inevitable, but they are not observed experimentally [3]. This is undoubtedly one of the reasons that the rt-KE is invoked to explain hollow particles, but a simple kinetic model shows that such pinholes should close quite quickly. The central physical observation is that without the pinhole, curvature variations on the surface are relatively small, but once the core has been dissolved away, there is a significant new driving force for mass transport from the convex outer surface to the concave inner one; this driving force distinguishes this problem from that of pinhole closure in planar films [17]. Mass transport occurs via surface diffusion, with the following general characteristics: In good approximation, the geometry of a shell with a pinhole is characterized by the mean curvature at three points (labeled A, B and C in Fig. 1). According to the Gibbs-Thomson relation, the chemical potential at each point is given by $\mu = \mu_\infty + \gamma\kappa\Omega$, where κ is the mean curvature as above, and μ_∞ is the reference chemical potential of a planar surface. Upon the formation of the pinhole, $\kappa_A = 1/R_0$ and $\kappa_C = -1/(R_0 - h)$, leading to an overall gradient in chemical potential that provides a driving force for mass transport from the outer surface to the inner one. At the pinhole edge $\kappa_B = (1/2)(1/a - 1/r)$, where r is the radius of the pinhole and $1/a$ is the curvature of the edge of the pinhole (Fig. 1). In principle, when the pinhole first opens, a may be very small, so that $\mu_B \gg \mu_A, \mu_C$ and the pinhole will open. However, his process will blunt the edge of the pinhole, quickly reducing the magnitude of a to a value of order of the shell thickness h. For small pinholes, the $1/r$ term then will dominate the chemical potential of the pinhole.

Next, we provide a simple analysis for the closure time of the pinhole. Quantitatively, if h is the shell thickness then the flux J^+ to the pinhole edge is

$$J^+ = -\frac{DC}{k_B T}\left[\frac{\mu_B - \mu_A}{\Delta x_1}\right] = -\frac{DC_{surf}\gamma\Omega^{2/3}}{k_B T}\left[\frac{1}{2}\left(\frac{1}{a} - \frac{1}{r}\right) - \frac{1}{R_0}\right]\frac{1}{(\pi R_0 - r)}. \tag{7}$$

7

This is a *minimum* flux, because we assume the distance Δx_1 over which the gradient is measured is maximal, equal to the distance from the pinhole edge to the point A on the particle farthest away from the edge, i.e., $\Delta x_1 = \pi R_0 - r$, and we have related the volumetric concentration of diffusers C to the surface concentration C_{surf} using $C_{surf} = C\Omega^{1/3}$. An expression similar to Eq. (7) can be written for the flux J^- between the pinhole edge and the inner surface using $\Delta x_2 = \pi\left(R_0 - h\right) - r$. For small enough a, one finds that the net flux $J_{net} = J^+ - J^-$ to the pinhole edge is always positive, consistent with the notion that pinholes should shrink. In the limit of small r/R_0 and h/R_0, this net flux is given by $J_{net} = \left[DC_{surf}\gamma\Omega^{2/3}/\left(\pi R_0 k_B T\right)\right]\left(1/r - 1/a\right)$. Mass conservation relates the shrinkage rate dr/dt of the pores to the net flux as $dr/dt = -J_{net}\Omega$, allowing us to determine the closure time t_c, i.e., the time elapsed during a change in pinhole radius from $r = r_0$ to $r = 0$:

$$t_c = \left(\frac{\pi a R_0 k_B T}{DC_{surf}\gamma\Omega^{5/3}}\right)\left(a\ln\left|\frac{a}{a - r_0}\right| - r_0\right). \tag{8}$$

Again, as we have taken the longest diffusion path possible, this expression is an approximate upper bound for the closure time. Figure 4 shows the closure time t_c versus initial pinhole radius r_0 for $R_0 = 6.5\ \text{nm}$ in shells comprised of Pt and PtO surfaces, for various values of the pinhole curvature a ($r_0 < a$). Pinholes in PtO-terminated surfaces close very quickly; except when the pinholes have radius greater than 1 nm, they will close up within of order 100 sec., i.e., shorter than any experiment. Pt terminated surfaces close more slowly, consistent with their smaller mobility, but even here we can expect pinholes of radius 0.5 nm to close up within of order 100 sec. As it is reasonable to approximate $a \approx h/2$, the data presented in [3], with a shell thickness of $h = 2$ nm, leads to a fast closure time of at most 100 sec., so our model is consistent with their observation that pinholes were not observed in *ex situ* microscopy after the end of the nanoparticle synthesis.

In this Letter, we have argued against the relevance of the room-temperature Kirkendall effect in core-shell nanoporous nanoparticles. Especially for the technologically relevant case of Pt nanoparticles, we showed that surface fluctuations are highly probable and lead to exposure of

nanoparticle cores. When these cores dissolve, any pinholes in the shell quickly close. The theory here is very robust in the sense that the same conclusions will be reached even assuming significant variation in any of the input parameters listed in Table 1. More broadly, this work confirms the dynamic nature of nanoparticle shape seen in microscopy and electrochemical measurements, and quantifies the degree to which thermal fluctuations can impact the stability and lifetime of structurally complex nanoparticles.

Acknowledgements

References

1. H.J. Fan, U. Gosele, and M. Zacharias, *Small* **3,** 1660 (2007).

2. A.M. Gusak and K.N. Tu, *Acta Materialia* **57**, 3367 (2009).

3. J.X. Wang, C. Ma, Y.M. Choi, D. Su, Y. Zhu, P. Piu, R. Si, M.B. Vukmirovic, Y. Zhang, and R.R. Adzic*, J. Amer. Chem. Soc.* **133**, 13551 (2011).

4. H.W. Pickering and C. Wagner, *J. Electrochem. Soc.* **114**, 698 (1967).

5. R.M. Emrick*, J. Phys. F* **12**, 1327 (1982).

6. D. Schumacher, A. Seeger, and O. Harlin, *Phys. Stat. Sol.* **25**, 359 (1968).

7. R. Callejas-Tovar, C. Alex Diaz, J. M. Martinez de la Hoz, and P.B. Balbuena, *Electrochim. Acta* (2013), http://dx.doi.org/10.1016/j.electacta.2013.01.053.

8. J. Erlebacher, M.J. Aziz, A. Karma, N. Dimitrov, and K. Sieradzki, *Nature* **410**, 450 (2001).

9. W.W. Mullins and R.F. Sekerka, *J. Appl. Phys.* **34**, 323 (1963).

10. L.D. Marks*, Rep Prog. Phys.* **57**, 603 (1994).

11. R. Rosso*, Interface Free Bound.* **3**, 345 (2001).

12. J. Cahn and J. Taylor, *Acta Metall. Mater.* **42**, 1045 (1994).

13. L. Tang, X. Li, R.C. Cammarata, C. Friesen, and K. Sieradzki, *J. Amer. Chem. Soc.* **132**, 11722 (2010).

14. J.J. Martinez Jubrias, M. Hidalgo, M.L. Marcos, J. Gonzalez Velasco, *Surf. Sci.* **366**, 239 (1996).

15. Martinez Jubrias, et al. [14] used slightly different numbers for surface energy and other physical parameters. They express the mobility $M = 2\gamma_A a^4 D_S' / k_B T$, where the lattice parameter $a = 0.39$ nm, $\gamma_A \left(= \gamma_{Pt} = \gamma_{PtO/Pt}\right) = 11.2$ eV/cm^2, and find an effective surface diffusivity D_S' that ranges from $1.5 x 10^{-18}$ (for Pt) to $16 x 10^{-18}$ cm^2 sec^{-1} (for PtO/Pt) in sulfate-based electrolytes. Equating this expression to ours, $M = C_{surf} D \Omega^2 \gamma / k_B T$, yields bounds for the product $C_{surf} D$ of $\sim 2.3 x 10^{-2}$ sec^{-1} (Pt) to $\sim 4.4 x 10^{-1}$ sec^{-1} (PtO/Pt).

16. L. Dubau, J. Durst, F. Maillard, L. Guetaz, M. Chatenet, J. Andre, and E. Rossinot, *Electrochim. Acta.* **56**, 10658 (2011).

17. M. Lanxner and C.L. Bauer*, Thin Solid Films* **150**, 323 (1987).

Table 1. Kinetic and Thermodynamic Parameters for Pt shell nanoparticle surfaces [13,14].

γ_{Pt} 15 eV/nm^2

$\gamma_{PtO/Pt}$ 3.1 eV/nm^2

Ω_{Pt} $1.5x10^{-2}$ nm^3

Ω_{PtO} $2.5x10^{-2}$ m^3

$\left(C_{surf} D \right)_{Pt}$ $2.3x10^{-2}$ sec^{-1} (~0.1 V vs. RHE)

$\left(C_{surf} D \right)_{PtO}$ $4.4x10^{-1}$ sec^{-1} (~1.1 V vs. RHE)
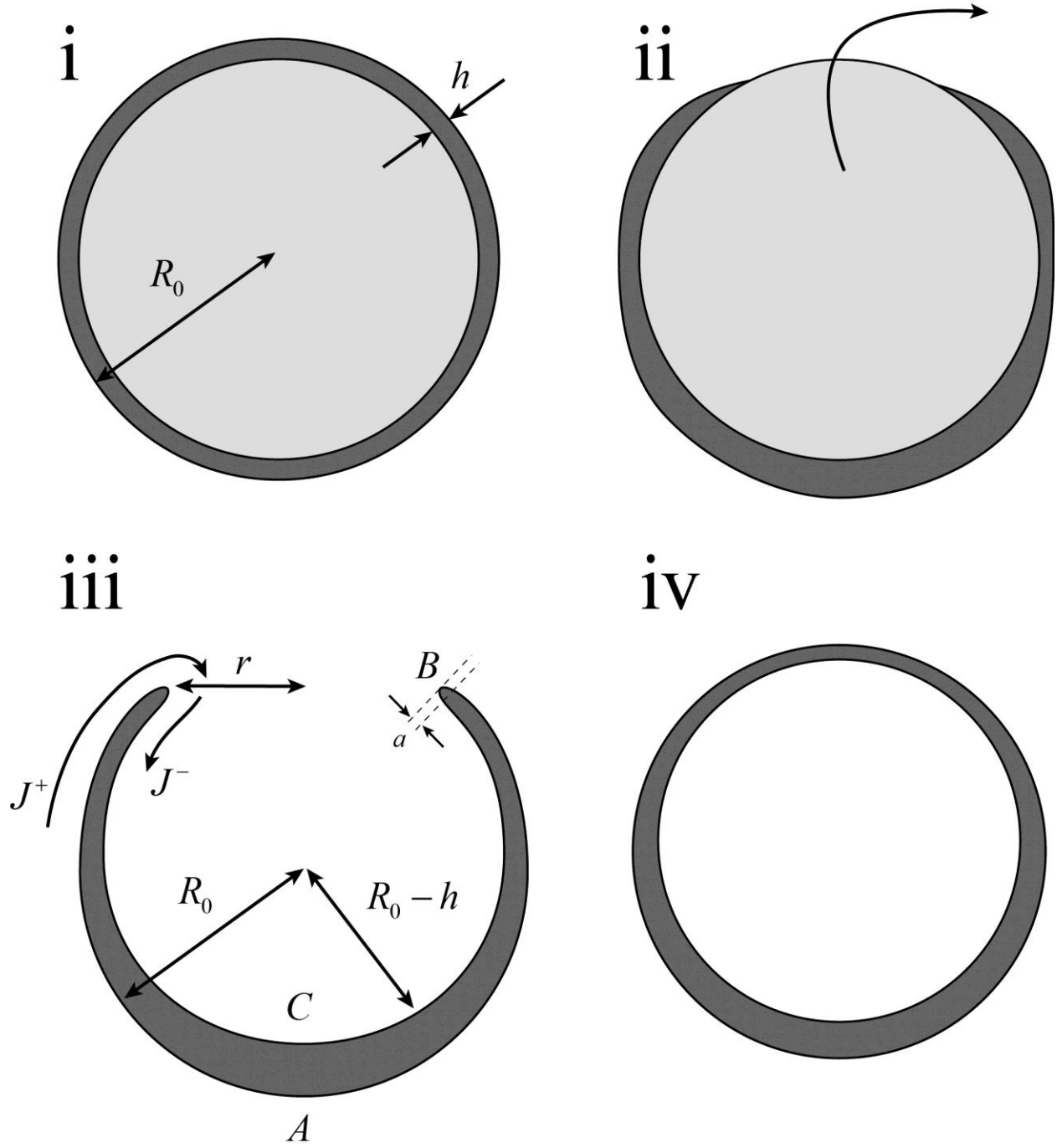
Figure 1. Stages in the surface-diffusion driven formation of hollow nanoparticles. (i) a core-shell nanoparticle of radius R_0 and shell thickness h; (ii) shape fluctuations in the outer surface expose the core, allowing it to be dissolved away; (iii) a pinhole of radius r exists in the shell, but quickly closes up because of a diffusional flux from the convex outer surface A through the pinhole edge B and into the inner concave surface C. (iv) When the radius of curvature of the pinhole edge a becomes sufficiently large, the net flux at the pinhole edge, $J^+ + J^-$ is positive, closing the pinhole and leaving a hollow nanoparticle.
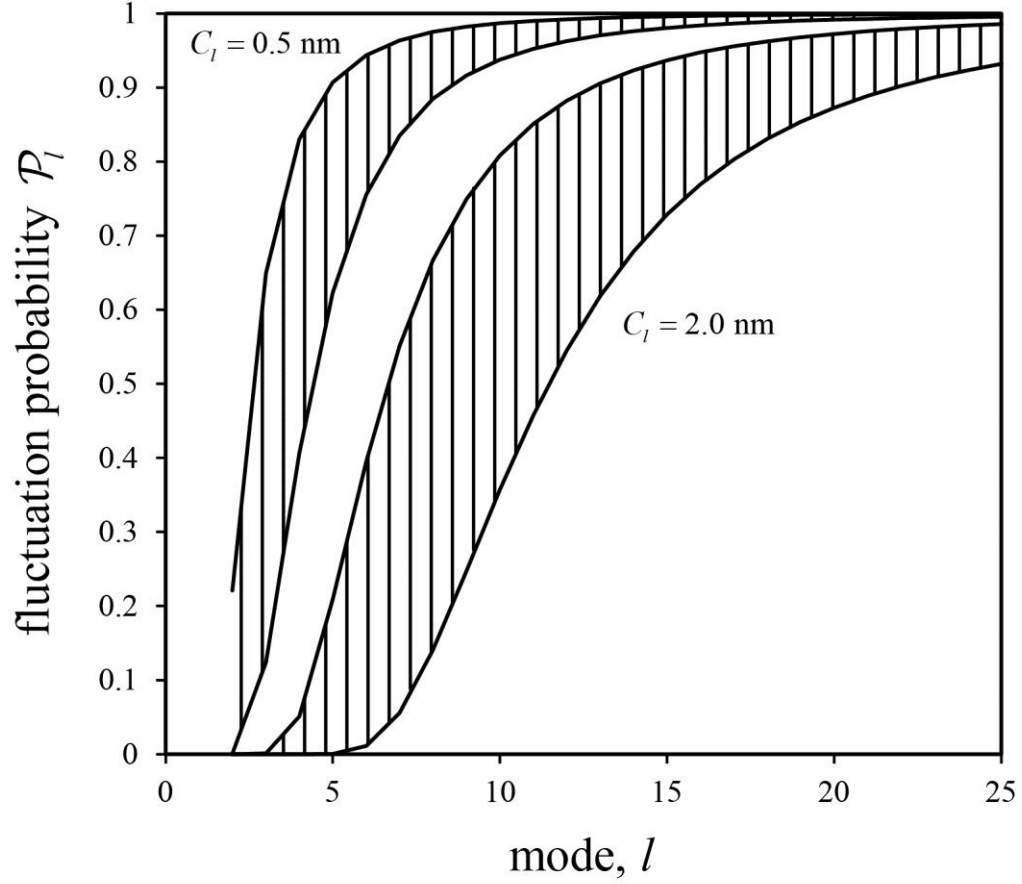
Figure 2. Fluctuation probability $\mathcal{P}_l$ versus fluctuation mode on $R_0 = 6.5$ nm Pt-shell nanoparticle surfaces: (upper shaded region) amplitude $C_l = 0.5$ nm; (lower shaded region) amplitude $C_l = 2.0$ nm. For each shaded region, the upper boundary is the probability on PtO-terminated surfaces, and the lower boundary is the probability on Pt-terminated surfaces.
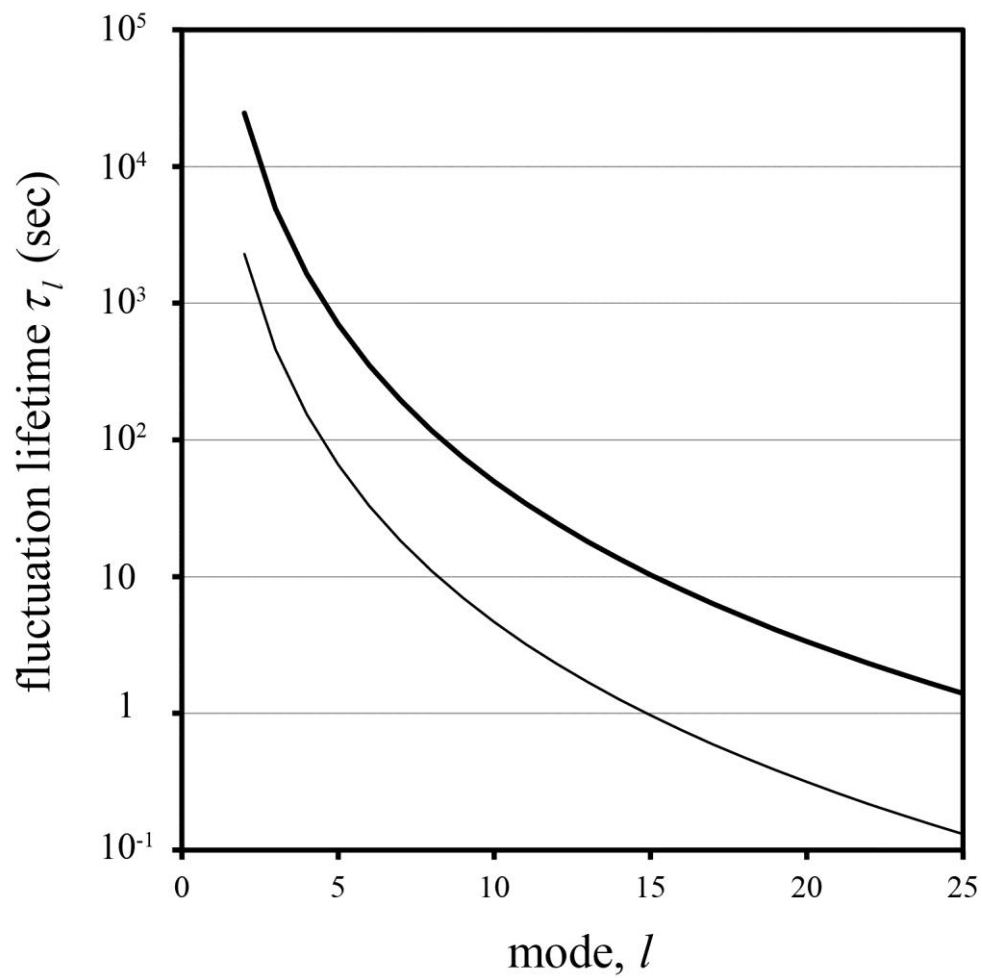
Figure 3. Fluctuation lifetime τ_l versus fluctuation mode l. (heavy line) Pt-terminated surfaces; (thin line) PtO-terminated surfaces.
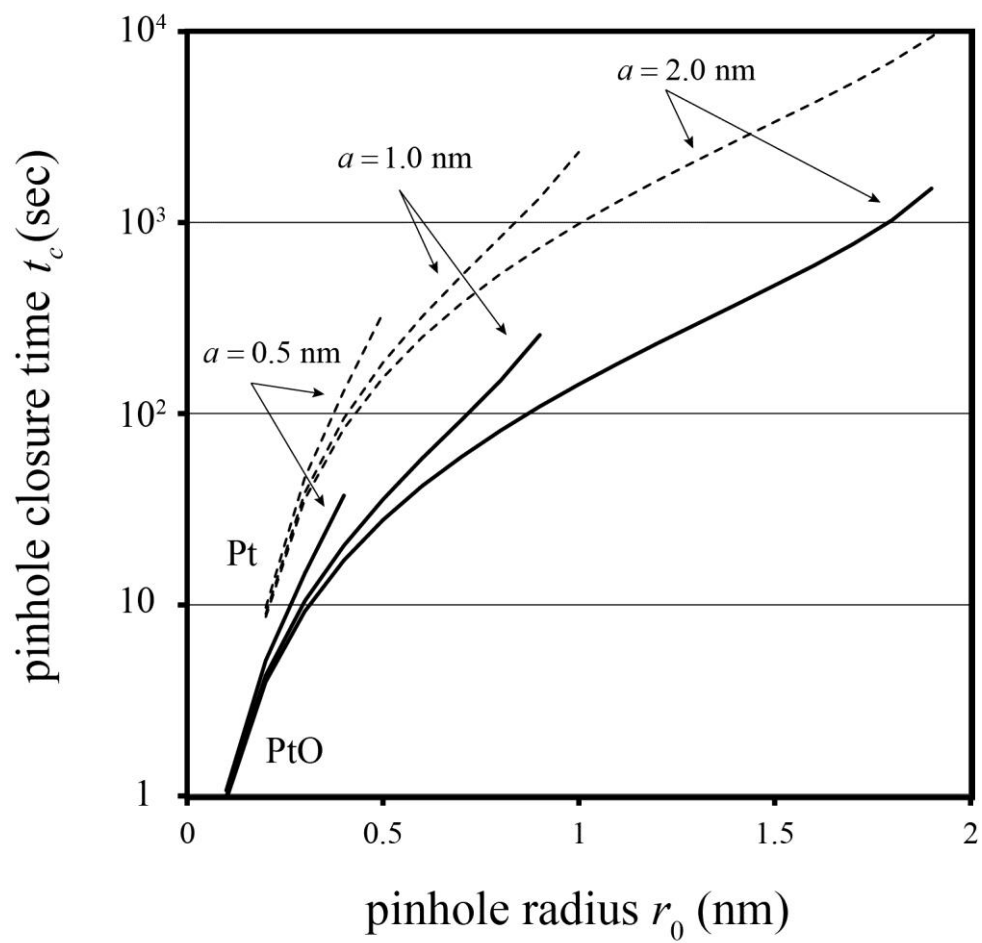
Figure 4. Pinhole closure time t_c versus initial pinhole radius r_0 for different values of the pinhole edge radius of curvature a. PtO-terminated surfaces: thick lines; Pt-terminated surfaces: thin dashed lines.